



Fermi National Accelerator Laboratory

FN-557
[E-687]

**Some Lifetimes and Branching Ratios
for Charmed Hadrons Produced in the
Fermilab Wide-Band Photon Beam ***

The E-687 Collaboration

presented by

W. D. Shephard
University of Notre Dame
Notre Dame, Indiana 46556

October 1990

* Presented at the XXVth International Conference on High Energy Physics, Kent Ridge, Singapore, August 2-8, 1990.



Operated by Universities Research Association Inc. under contract with the United States Department of Energy

Some Lifetimes and Branching Ratios for Charmed Hadrons Produced in the Fermilab Wide-Band Photon Beam

P.L. Frabetti

Dip. di Fisica dell'Universita' and INFN - Bologna, I-40126 Bologna, Italy

C.W. Bogart, H. Cheung, P. Coteus,^(a) S. Culy, J.P. Cumalat, D. Kaplan^(b)
University of Colorado, Boulder, CO 80309, USA

J. Butler, F. Davenport,^(c) I. Gaines, P. Garbincius, S. Gourlay, D. Harding,
P. Kasper, A. Kreymer, P. Lebrun, H. Mendez,
Fermilab, Batavia, IL 60510, USA

S. Bianco, M. Enorini, F.L. Fabbri, A. Spallone, A. Zallo
Laboratori Nazionali di Frascati, I-00044 Frascati, Italy

R. Culbertson, M. Diesburg,^(d) G. Jaross, K. Lingel, P. Sheldon, J.R. Wilson,
J. Wiss
University of Illinois at Urbana-Champaign, Urbana, IL 61801, USA

G. Alimonti, G. Bellini, M. Di Corato, M. Giammarchi, P. Inzani, S. Malvezzi,
P.F. Manfredi,^(c) D. Menasce, E. Meroni, L. Moroni, D. Pedrini, L. Perasso,
F. Ragusa, A. Sala, S. Sala, D. Torretta, M. Vittone^(d)
Dip. di Fisica dell'Universita' and INFN - Milano, I-20133 Milan, Italy

D. Buchholz, C. Castoldi,^(f) B. Gobbi, S. Park, R. Yoshida
Northwestern University, Evanston, IL 60208, USA

J.M. Bishop, J.K. Busenitz,^(g) N.M. Cason, J.D. Cunningham, R.W. Gardner,
C.J. Kennedy, E.J. Mannel, R.J. Mountain, D.L. Pusejic, R.C. Ruchti,
W.D. Shephard, M.E. Zanabria
University of Notre Dame, Notre Dame, IN 46556, USA

G.L. Boca, R. Diaferia, S.P. Ratti, P. Vitulo
Dip. di Fisica dell'Universita' and INFN - Pavia, I-27100 Pavia, Italy

A. Lopez

University of Puerto Rico at Mayaguez, Puerto Rico

Presented by W.D. Shephard for the Fermilab E687 Collaboration

Abstract

Preliminary values are presented for lifetimes of the Λ_c^+ decaying into $pK^-\pi^+$ and D_s^+ decaying into $\phi\pi$. Also presented are preliminary results on samples of $D^0 \rightarrow \bar{K}^0 K^+ K^-$, including $D^0 \rightarrow \bar{K}^0 \phi$, and $D^0 \rightarrow \bar{K}^0 \pi^+ \pi^-$ decays. The data are from the first run of Fermilab experiment E687 using the Fermilab Wide-Band Photon Spectrometer. Our lifetime values are $(0.20 \pm 0.03 \pm 0.03)$ ps for the Λ_c^+ and $(0.50 \pm 0.06 \pm 0.03)$ ps for the D_s^+ . We find preliminary values for the branching ratios $B(D^0 \rightarrow \bar{K}^0 K^+ K^-)/B(D^0 \rightarrow \bar{K}^0 \pi^+ \pi^-)$ and $B(D^0 \rightarrow \bar{K}^0 \phi)/B(D^0 \rightarrow \bar{K}^0 \pi^+ \pi^-)$ of 0.20 ± 0.06 and 0.16 ± 0.06 , respectively; only statistical errors are quoted. Further work is in progress..

Introduction

While much is now known about the properties of charmed hadrons [1] [2], there is still much we need to learn. Fermilab experiment E687 is a high-statistics study of photoproduced hadronic interactions using the highest-energy photon beam currently available. It will provide new information on a number of aspects of charmed hadron production over the next few years. Preliminary results from the first run of E687 in which about 60 million γ Be triggers (about 75% hadronic) were recorded on tape are now becoming available. Final samples from this first run are expected to include about 10^4 reconstructed charm decays in all. The current second run of E687 is expected to provide more than 5 times more data for future analysis.

The results presented here demonstrate applications of candidate-driven charm selection algorithms to the E687 first-run data sample; candidate track combinations for specific hypotheses are used as seeds for vertex location. Presented are preliminary E687 results for several charmed particle lifetimes. These include the Λ_c^+ and D_s^+ lifetimes which are currently known with less precision than D^+ and D^0 lifetimes where the event samples are larger. In the analyses reported here and in other E687 lifetime analyses reported at this conference[3], various fitting schemes have been employed. Studies are in progress to determine the most appropriate algorithms and the associated systematic uncertainties in each case. Also presented are preliminary results of studies on branching ratios and branching fractions. Of special interest are $D^0 \rightarrow K_S^0 K^+ K^-$ decays. For example, the decay $D^0 \rightarrow \bar{K}^0 \phi$ is proposed as a test of nonspectator decay processes [4]. More information is expected on all these topics by the time of this conference.

The Fermilab Wide-Band Photon Spectrometer used for E687 is a two-magnet spectrometer with large acceptance for charged and neutral hadrons and for muons, electrons, and photons. Both electromagnetic and hadronic calorimeters are included in the spectrometer. The charged particles are traced with 4 silicon microstrip stations having 3 planes each and 5 multiwire proportional chambers having 4 planes

each. Charged particles are identified with 3 multicell Čerenkov detectors having pion thresholds of 4.4, 6.7, and 17 GeV/c. The system provides unique identification of kaons from 17 to 45 GeV/c and protons from 17 to 45 GeV/c and 60 to 117 GeV/c and identification of “heavy” (K/p ambiguous) particles from 45 to 60 GeV/c. Details of the spectrometer and its capabilities are presented elsewhere [3] [5][6][7]. The bremsstrahlung photon beam was obtained from 350 GeV/c electrons with a 13% momentum spread impinging on a 27% radiator. The photons were tagged by detection of the recoil electron. The beam was incident on a Be target for most of the first run. The data were taken with a trigger demanding at least two tracks in the spectrometer, both required to be outside the pair production region, and an energy deposit larger than a specified minimum value (typically about 40 GeV) in the hadron calorimeter. The average photon energy for hadronic triggers was 221 GeV.

Λ_c^+ Lifetime

The charmed baryon Λ_c^+ lifetime is particularly difficult to measure since it is shorter than charmed meson lifetimes. Cuts on the significance of separation between production and decay vertices reject larger portions of the signal. Also the Λ_c^+ is typically produced at a lower rate and lacks dominant low-multiplicity all-hadronic decay modes. This lifetime measurement was made with a sample of $\Lambda_c^+ \rightarrow pK^-\pi^+$ decays.

The sample was obtained with a candidate-driven vertex finder using the silicon microstrip data. Combinations of three tracks consistent with the hypothesis $\Lambda_c^+ \rightarrow pK^-\pi^+$ were first selected. (In every case the equivalent candidate combinations for the Λ_c^+ were also considered.) All candidate tracks were required to be reconstructed in the main spectrometer tracking system and successfully linked to a microstrip track candidate. Tracks consistent with a muon hypothesis were rejected. The proton and pion candidates were required to have the same charge and the kaon candidate was required to have the opposite charge. Čerenkov cuts were applied. The proton track must be identified as a proton or K/p ambiguous; the kaon must be identified as a kaon or K/p ambiguous. If both proton and kaon were ambiguous then the combination was rejected. The pion track must not be identified as electron, kaon, proton or K/p ambiguous. The vertex algorithm was applied to the candidate track combinations as follows. First a secondary vertex was formed from the three selected tracks with the requirement that the χ^2 per degree of freedom for the global vertex fit be less than 3.0. Next a seed track was constructed from the momentum vectors of the charm candidate daughter tracks. Other tracks that intersect the seed track were used to make a primary vertex. In this fashion one or more additional tracks may be included. The final global fit for the primary vertex was required to have $\chi^2/\text{DOF} < 3.0$. No tracks other than the three candidates could be consistent with the secondary vertex. Finally the distance, L ,

between the secondary and primary vertex was calculated and divided by the error on that difference, σ_L . Typical errors on this distance, when converted to proper time, were about 0.04 ps for the Λ_c^+ candidates. For the final Λ_c^+ sample the cut on the significance of the vertex separation was $L/\sigma_L > 3.0$. The primary vertex was also required to lie in the target region.

Cuts were also employed on the cosine of the angle between each daughter track in the Λ_c^+ rest frame and the Λ_c^+ momentum vector in the laboratory frame. The cosine was defined as

$$\cos \theta = \frac{p_{\parallel}}{((p_{\parallel})^2 + (p_{\perp}^2))^{\frac{1}{2}}}.$$

The cuts were $\cos \theta < 0.9$ for the pion, $\cos \theta > -0.9$ for the kaon, and $-0.9 < \cos \theta < 0.9$ for the proton. These cuts eliminated low momentum background with large production angles. Finally an additional cut required each Λ_c^+ to have an energy greater than 70 GeV. This energy cut further reduced the background. The average efficiency for reconstructing this Λ_c^+ decay mode with all cuts is estimated to be about 5.8%.

In Fig. 1 is shown the combined mass distribution for accepted $pK^-\pi^+$ and charge conjugate combinations after all the above cuts. The solid curve is a fit with a Gaussian signal plus a quadratic background. The fit yields a signal with 90 ± 17 events at a mass of $2283 \pm 4 \text{ MeV}/c^2$. Fits to individual particle and antiparticle plots yield 50 ± 12 and 51 ± 17 event signals respectively.

The Λ_c^+ lifetime determination used an event-by-event maximum-likelihood fit to the distribution of proper time corrected for the L/σ_L cut, $t' = (L - 3.0\sigma_L)/\beta\gamma c$, where L is the separation between primary and secondary vertices. The minimum t' is 0.0 and the maximum t'_{max} is determined on an event-by-event basis requiring that the Λ_c^+ decay occur upstream of a trigger counter just in front of the first microstrip plane.

A combined fit of signal and background was made for combinations with mass between 2.10 and 2.45 GeV/c^2 . The mass distribution was described with a Gaussian signal term and a quadratic polynomial background term. The mass fit parameters were fixed at values from a fit to the mass histogram alone. Preliminary studies of the proper time distribution of the background were made using mass sideband regions above and below the mass of the Λ_c^+ . Fits of various functions were made to the the proper time distributions for the background regions. Single-exponential and Gaussian functions did not provide an adequate description. Using double exponential functions, good fits could be obtained with parameters consistent with being mass-independent. Monte Carlo event samples with no charm component and with the same cuts as the data could also not be described well by single-exponential and Gaussian functions but could be fitted well with double exponential functions. The study indicates that the background is consistent with tracks produced at the

primary vertex whose reconstruction is consistent with originating at a secondary vertex due to resolution effects.

For the final fit, the following function, properly normalized event by event over the allowed t' and mass ranges, was maximized:

$$\mathcal{L} = \sum_{i=1}^N \log(S_i + B_i)$$

where the unnormalized signal and background functions were

$$S_i = \frac{A}{\sigma\sqrt{2\pi}} \exp \frac{-(m_i - \bar{m})^2}{2\sigma^2} \frac{f(t'_i)}{\tau} \left(\exp \frac{-t'_i}{\tau} \right)$$

$$B_i = g(m_i) (\exp(-t'_i/\tau_{B_1}) + C \exp(-t'_i/\tau_{B_2})).$$

The linear function $f(t'_i) = F + Gt'_i$ in S_i includes the effects of spectrometer acceptance and of secondary-particle absorption in the target as a function of t' . It was determined from Monte Carlo studies. A quadratic function $g(m_i)$ was used to describe the background mass distribution in B_i .

The Λ_c^+ lifetime from the final fit is 0.20 ± 0.03 ps. The fitted values in the background parameterization are $\tau_{B_1} = 0.10$ ps, $\tau_{B_2} = 1.75$ ps, and $C = 0.25$. Figure 2 shows the t' distribution for the final sample, integrated over the mass range, together with the fitted curve.

A study was made using different L/σ_L cuts to look for systematic effects due to correlations; no such effects were found. As an additional check, the lifetime was also determined with a binned maximum likelihood fit using a sideband background subtraction procedure similar to that used by Anjos *et al.* [8]. This fit yielded a Λ_c^+ lifetime consistent with the value quoted above. Inclusion of the correction function $f(t')$ consistently reduced the lifetime by 0.02 ps in both types of fits compared to fits without this factor. The systematic error for the Λ_c^+ lifetime is still under study with fits made using different algorithms and background parameterizations and with Monte Carlo simulations; a preliminary estimate of the systematic uncertainty is 0.03 ps. Most of the analysis to obtain the final Λ_c^+ sample has been done by C. W. Bogart of the University of Colorado. More details are given in his Ph.D. thesis [9].

The world average for the Λ_c^+ lifetime determined in 1988 by the Particle Data Group [1] was $0.179^{+0.023}_{-0.017}$ ps. Anjos *et al.* [8] in 1988 published a value of $0.22 \pm 0.03 \pm 0.02$ using a sample of photoproduced Λ_c^+ 's. Our preliminary value of $0.20 \pm 0.03 \pm 0.03$ ps is quite consistent with both of these values.

D_s^+ Lifetime

A preliminary result for the D_s^+ lifetime has been determined using a sample of $\phi\pi^+$ decays of the D_s^+ with $\phi \rightarrow K^+K^-$. (Charge conjugate states are included.) The mass distribution for K^+K^- combinations where both tracks are required to be Čerenkov consistent with the kaon hypothesis shows a clear ϕ peak as seen in Fig. 3. A fit to this distribution with a P-wave Breit-Wigner signal function and a second-order polynomial background yields about 100,000 ϕ 's with a mean mass of $1019.54 \pm 0.02 \text{ MeV}/c^2$ and a width of $6.1 \pm 0.1 \text{ MeV}/c^2$; this mass is quite close to the accepted value[1]. All ϕ candidates with K^+K^- masses of $1020 \pm 10 \text{ MeV}/c^2$ were selected for the D_s^+ analysis.

The sample was obtained in a manner similar to that described for the Λ_c^+ case. The K^+ and K^- tracks from the ϕ candidates described above were combined with single tracks identified in the Čerenkov system as consistent with the pion hypothesis to form the initial three-track combinations for vertex fitting. The χ^2 per degree of freedom for the $K^+K^-\pi^+$ secondary vertex was required to be less than 3.0. Again the momentum vector resulting from these three tracks was used as a seed for the primary vertex. The primary vertex was required to be in the target region and the secondary vertex was required to be downstream of the primary vertex. Unlike the Λ_c^+ analysis, there was no requirement that the individual tracks be muon inconsistent or that the state energy be within certain limits. However an additional cut was made. For the decay $D_s^+ \rightarrow \phi\pi^+$, the distribution for the angle between the K^+ and the π^+ , when viewed in the ϕ rest frame is expected to be $dN/d\cos\theta \propto (\cos\theta)^2$. The forward/backward peaking in the $\cos\theta$ distribution can be exploited to improve the signal-to-background ratio in the D_s^+ analysis since our spectrometer has flat acceptance in θ . For the D_s^+ analysis, a cut of $|\cos\theta| \geq 0.3$ was used. This cut retained 97% of the signal while removing about 30% of the background.

The $\phi\pi$ mass distributions for various cuts on the significance, L/σ_L , of the vertex separation were studied. Figure 4 shows four plots of $\phi\pi$ mass with different cuts on L/σ_L . Two prominent peaks are present. The higher-mass peak corresponds to the D_s^+ and the lower to the Cabibbo-suppressed decay of the D^+ . It is quite evident that as L/σ_L is increased the peak for the longer-lived D^+ becomes increasingly larger relative to the D_s^+ peak.

For the final sample used in the D_s^+ lifetime determination, a cut of $L/\sigma_L > 3.0$ was imposed. A fit to the corresponding mass distribution with a function including two Gaussian signals and a background term linear in mass yields the following signal parameters: for the D_s^+ peak the mass is $1967 \pm 2 \text{ MeV}/c^2$ with $\sigma = 11.1 \pm 2.6 \text{ MeV}/c^2$ and the yield is 104 ± 15 events; for the D^+ peak the mass is $1871 \pm 3 \text{ MeV}/c^2$ with $\sigma = 7.4 \pm 3.7 \text{ MeV}/c^2$ and the yield is 50 ± 10 events. The fitted masses are

consistent with the accepted values [1].

The D_s^+ lifetime reported here was determined using an event-by-event maximum-likelihood fit of a function similar to that used in the Λ_c^+ analysis. However, the likelihood function \mathcal{L} differed from that for the Λ_c^+ in several ways. The proper time $t = L/(\beta\gamma c)$ (unmodified for the L/σ_L cut) was used as the fit variable rather than $t' = (L - 3.0\sigma_L)/\beta\gamma c$.

The signal function S_i contained two terms, the first term for the D_s^+ decay and the second for the Cabibbo-suppressed decay of the D^+ :

$$S_i = \frac{N_1}{\sigma_1\sqrt{2\pi}} \exp \frac{-(m_i - m_1)^2}{2\sigma_1^2} \frac{f(t_i)}{\tau_1} \left(\exp \frac{-t_i}{\tau_1} \right) + \frac{N_2}{\sigma_2\sqrt{2\pi}} \exp \frac{-(m_i - m_2)^2}{2\sigma_2^2} \frac{f(t_i)}{\tau_2} \left(\exp \frac{-t_i}{\tau_2} \right)$$

The function $f(t)$ is a correction function including the effects of acceptance as a function of proper time and of secondary particle absorption in the target. This function was determined on the basis of Monte Carlo studies and was parameterized as a second order polynomial in t .

Studies of the background were performed [10] using four mass sideband regions, two above and two below the mass region containing the D_s^+ and D^+ mass peaks. Fits were made to the distributions in proper time $t = L/(\beta\gamma c)$ for the various background regions. Again, single-exponential and Gaussian functions did not adequately describe the background proper time distributions but good fits could be obtained with a double exponential function. The parameters τ_{B_1} , τ_{B_2} and C determined from these fits were consistent with being mass-independent. The double exponential form is consistent with the resolution in proper time expected from Monte Carlo studies. The form of the function B_i used in the final fit was

$$B_i = g(m_i) \left(\exp(-t_i/\tau_{B_1}) + C \exp(-t_i/\tau_{B_2}) \right).$$

A linear polynomial function, $g(m_i)$, was sufficient to fit the background mass contribution. Initial values for the background parameters τ_{B_1} , τ_{B_2} and C were obtained from fits to the background regions and were also tested on Monte Carlo data samples with no charm component. The parameters were then allowed to vary in the final fit; the final values $\tau_{B_1} = 0.11 \pm 0.01$ ps, $\tau_{B_2} = 0.53 \pm 0.07$ ps, and $C = 0.14 \pm 0.03$ still adequately described the background regions.

The fit functions S_i and B_i were normalized over mass and proper time. For mass, they were normalized over the total mass range from 1.7 to 2.1 GeV/c², while for proper time t they were normalized on an event-by-event basis over the range t_{min} to t_{max} . The value of t_{min} was $3\sigma_{L_i}/(\beta\gamma c)$, while t_{max} was determined by the requirement that the decay occur upstream of a trigger counter just upstream of

the first microstrip plane. It is not possible to accurately determine vertex positions downstream of the first silicon microstrip plane. However, the trigger counter is sufficiently far from the target that very few D_s^+ decays are expected beyond this point.

The fit yielded a value of 0.50 ± 0.06 ps for the D_s^+ lifetime. The fitted lifetime for the Cabibbo-suppressed D^+ was 0.90 ± 0.13 ps. If the same type of fit is done without the correction function (i.e. $f(t)$ is set equal to 1.0) the resulting lifetime values are 0.53 ± 0.07 ps for the D_s^+ lifetime and 1.09 ± 0.19 ps for the D^+ lifetime. Figure 5 shows a distribution in proper time t for events in the narrow D_s^+ mass region from 1.94 to 1.99 GeV/c² together with the curve corresponding to the fit. Further studies of systematic uncertainties are in progress. Preliminary estimates of the systematic uncertainty are ± 0.03 ps and ± 0.10 ps for the D_s^+ and D^+ , respectively. Much of this analysis on the D_s^+ lifetime has been performed by J. D. Cunningham of the University of Notre Dame.

Our preliminary lifetime values of $0.50 \pm 0.06 \pm 0.03$ ps for the D_s^+ and $0.90 \pm 0.13 \pm 0.10$ ps for the D^+ may be compared with recently published values. Our preliminary value for the D_s^+ lifetime is somewhat larger than (although not inconsistent with) the world average of $0.436_{-0.032}^{+0.038}$ ps. given in Ref. [1]; it is still closer to the more recent average value of 0.46 ± 0.04 ps. quoted in Ref. [2]. Our preliminary value for the D^+ lifetime is somewhat lower than the average values of $1.069_{-0.032}^{+0.031}$ ps. and 1.082 ± 0.032 ps. from Refs. [1] and [2], respectively, but is of low statistical significance due to the limited statistics available for the Cabibbo-suppressed $D^\pm \rightarrow \phi\pi$ decay modes. Preliminary lifetime values of greater statistical significance obtained using data from Fermilab E687 for other decay modes of the charged and neutral D mesons are given in Ref. [3]; the values for the D^+ are consistent with the averages cited above.

Branching Ratios for Charm Decays

Measurements of the decay rates for the many decay modes of the charmed mesons can, in principle, provide valuable tests of the mechanisms for decay. Many decay modes have already been observed and values for many branching ratios have been determined. But the errors on many of these determinations are still substantial; there is a need for all the additional information we can get. E687 is a potential source of much information on the subject. Obtaining final values is not a simple task. The first step of determining branching ratios requires careful estimates of detection efficiencies for different modes. The ratios often are quite sensitive to such factors as the Čerenkov identification efficiencies for kaons. Measurement of absolute branching fractions is still more difficult, since an absolute normalization is needed in addition. E687 now has good samples of many decay modes of the charmed mesons. The study of relative detection efficiencies is well under way in

several cases and results for various branching ratios are expected to be available by the time of this conference. Initial estimates of branching fractions can be made by using other published results; measurements of branching fractions based entirely on E687 results will follow.

Presented here, as an example of the work in progress, are preliminary results on $D^0 \rightarrow K_S^0 K^+ K^-$ and $D^0 \rightarrow K_S^0 \pi^+ \pi^-$ decays reconstructed in the spectrometer. Of special interest is the decay $D^0 \rightarrow \bar{K}^0 \phi$ since it can serve as a test for the presence of non-spectator decay processes[4]. The situation has been summarized in Ref. [2]. The average value of the branching fraction $B(D^0 \rightarrow \bar{K}^0 \phi)$ from three experiments [11][12][13] was $(0.83^{+0.18}_{-0.16})\%$. A recent report on decay modes of charmed particles from CERN NA32[14] lists a still larger value for this branching fraction, although with rather large uncertainty: $B(D^0 \rightarrow \bar{K}^0 \phi) = (1.70 \pm 0.58)\%$. This rate is rather large, considering the need for producing an additional $s\bar{s}$ pair. The effect was initially interpreted as due to annihilation decays, but it has also been ascribed to rescattering effects in final states produced by spectator decay. Calculations using QCD sum rules by Blok and Shifman [15] and the factorization approach of Bauer, Stech, and Wirbel [16] have yielded predictions of about the same size branching fraction as has been measured; the $1/N$ phenomenology of Buras, Gerard, and Ruckl [17] predicts smaller values. A better understanding of the mechanism of this decay may require better measurements as well as better results on other non-spectator decays of the D^0 and D_s^+ . E687 should provide some of these results.

Samples of the decays $D^0 \rightarrow K_S^0 K^+ K^-$ and $D^0 \rightarrow K_S^0 \pi^+ \pi^-$ have been extracted from the E687 first-run data. The latter decay is more likely and thus statistical errors on that sample are smaller; it will be used as the reference for branching ratio determinations. The $K_S^0 \pi^+ \pi^-$ system is sufficiently similar to the $K_S^0 K^+ K^-$ system that most systematic effects should tend to cancel in ratios. However, studies of corrections involving the detection and identification efficiencies for charged kaons and pions must be completed before final branching ratios can be presented. Preliminary results will be presented here.

The starting point for this analysis is a sample of events containing about 10^6 reconstructed K_S^0 mesons which decay between the target and the first proportional wire chamber in the spectrometer (just downstream of the first magnet). In Fig. 6 is shown the K_S^0 mass distribution for the sample used for $K_S^0 K^+ K^-$ and $K_S^0 \pi^+ \pi^-$ event selection. The fitted K_S^0 mass is $497.1 \text{ MeV}/c^2$ and the width is $5 \text{ MeV}/c^2$.

In selecting candidates for $D^0 \rightarrow K_S^0 K^+ K^-$ and $D^0 \rightarrow K_S^0 \pi^+ \pi^-$ decays, the candidate K_S^0 mesons were required to satisfy a number of criteria including cuts on the reconstructed mass and on the K_S^0 vertex fit. For $D^0 \rightarrow K_S^0 K^+ K^-$ decay candidates, the charged kaon candidate tracks were required to be Čerenkov consis-

tent with the kaon hypothesis; for $D^0 \rightarrow K_S^0 \pi^+ \pi^-$ decay candidates, no Čerenkov identification requirements were placed on the pion candidates. In both cases the invariant mass of the three-particle system was required to be in the range 1.6 to 2.1 GeV/c². The primary and secondary vertices were reconstructed in a manner similar to that previously described. Confidence level cuts were made on the vertex fits. The primary vertex was required to include at least two tracks in addition to the seed track. L/σ_L cuts were then applied to select the final samples. In selecting the $K_S^0 \pi^+ \pi^-$ sample, a stringent cut of $L/\sigma_L > 10.0$ was applied in order to improve the signal-to-background ratio. For the smaller $K_S^0 K^+ K^-$ sample a cut of $L/\sigma_L > 3.0$ was used to provide an adequate signal-to-background ratio while still yielding a signal of reasonable size. Studies are being made to check for possible systematic effects associated with the L/σ_L cuts. As a final cut, the momenta of the D^0 candidates in each sample were restricted to be between 45 and 160 GeV/c². This ensured that the candidates have momenta in a region where spectrometer acceptance was good.

The resulting mass distributions are shown in Fig. 7. Superimposed on the distributions are curves for fits with a Gaussian signal plus a polynomial background. For the $K_S^0 \pi^+ \pi^-$ case a linear background provided a good fit; for the $K_S^0 K^+ K^-$ case a quadratic background was needed. The D^0 signal parameters for both decay modes are shown in Table 1. The fitted masses are consistent with the accepted D^0 mass value of 1864.5 MeV/c² from Ref. [1].

Table 1. D^0 Signal Parameters.

parameter	$K_S^0 \pi^+ \pi^-$	$K_S^0 K^+ K^-$
Yield	215 ± 28	35.2 ± 8.8
Mass	$1863.5 \pm 2.0 \text{ MeV}/c^2$	$1867.4 \pm 1.7 \text{ MeV}/c^2$
Width	$13.5 \pm 2.0 \text{ MeV}/c^2$	$5.7 \pm 1.8 \text{ MeV}/c^2$
Signal/Noise	0.8	0.9

In order to compute branching ratios, the raw experimental distributions must be weighted to account for spectrometer acceptance, and for reconstruction and particle identification efficiencies. Acceptance functions have been determined as a function of D^0 momentum for each of the samples. Monte Carlo samples of events were generated and binned in momentum intervals small enough so that the variation in acceptance is not too large within a bin. The Monte Carlo events were reconstructed with the same programs and subjected to the same cuts as the data. The distributions of the fraction of events in each bin which survive are fitted with polynomial

curves to determine overall acceptance functions. Each real event is then weighted by the inverse of the acceptance function evaluated at the appropriate momentum. The weighted mass distributions can then be fitted in the same manner as the raw data distributions and the resulting fitted D^0 signal parameters can be used to determine the inclusive branching ratio $B(D^0 \rightarrow \overline{K}^0 K^+ K^-) / B(D^0 \rightarrow \overline{K}^0 \pi^+ \pi^-)$.

For the $D^0 \rightarrow K_S^0 \pi^+ \pi^-$ sample the efficiency determined from the Monte Carlo studies for the $L/\sigma_L > 10.0$ cut peaks at about 7% and varies by no more than a factor of 3 to 4 over the D^0 momentum range chosen for the real event samples. For the $D^0 \rightarrow K_S^0 K^+ K^-$ sample the efficiencies for charged kaon identification as a function of momentum are still under study. Event weights for the following preliminary estimates of branching ratios have been determined by combining weights from a Monte Carlo sample without the Cerenkov cuts with individual weights for charged kaon identification efficiency determined from empirical studies of samples of D^0 and D^\pm mesons with decay modes including single charged kaons. The resulting weights vary over the chosen D^0 momentum range by factors comparable to those for the $D^0 \rightarrow K_S^0 \pi^+ \pi^-$ sample listed above. The weighted mass distributions have been fitted in the same manner as the unweighted distributions. The distributions and fitted curves are shown in Fig. 8 and the preliminary weighted D^0 signal parameters are shown in Table 2.

Table 2. Weighted D^0 Signal Parameters.

parameter	$K_S^0 \pi^+ \pi^-$	$K_S^0 K^+ K^-$
Yield	4370 ± 660	860 ± 220
Mass	$1861.9 \pm 2.1 \text{ MeV}/c^2$	$1867.7 \pm 2.0 \text{ MeV}/c^2$
Width	$13.1 \pm 2.6 \text{ MeV}/c^2$	$7.0 \text{ MeV}/c^2$ fixed
Signal/Noise	0.6	0.8

The inclusive branching ratio $B(D^0 \rightarrow \overline{K}^0 K^+ K^-) / B(D^0 \rightarrow \overline{K}^0 \pi^+ \pi^-)$ is simply taken as the ratio of the weighted yields. The preliminary result, with statistical errors only, is:

$$\frac{B(D^0 \rightarrow \overline{K}^0 K^+ K^-)}{B(D^0 \rightarrow \overline{K}^0 \pi^+ \pi^-)} = \frac{N(D^0 \rightarrow K_S^0 K^+ K^-)}{N(D^0 \rightarrow K_S^0 \pi^+ \pi^-)}$$

$$= 0.20 \pm 0.06$$

This value may be compared with the world average [1] of 0.20 ± 0.05 . The values of the branching fraction for $D^0 \rightarrow \bar{K}^0 \pi^+ \pi^-$ of $5.6_{-0.6}^{+0.7}\%$ from Ref. [1] and $6.4 \pm 0.4\%$ from the Mark III Collaboration [18] can be combined with our branching ratio to give preliminary values for the absolute branching fraction for $D^0 \rightarrow \bar{K}^0 K^+ K^-$ of $1.10 \pm 0.35\%$ and $1.26 \pm 0.38\%$ respectively.

In Fig. 9a is shown a two-dimensional scatter plot of $K^+ K^-$ mass as a function of the candidate $K_S^0 K^+ K^-$ mass for the total $K_S^0 K^+ K^-$ sample. Also shown in Figs. 9b and 9c are the corresponding unweighted $K_S^0 K^+ K^-$ and $K^+ K^-$ mass distributions. The D^0 can be seen in the scatter plot and the corresponding mass peak can be seen in the $K_S^0 K^+ K^-$ mass distribution. A clear ϕ band can be seen in the scatter plot and the ϕ mass peak can be seen at about $1020 \text{ MeV}/c^2$ in the $K^+ K^-$ mass plot. There appears to be an enhancement where the bands overlap on the scatter plot. To determine the fraction of $D^0 \rightarrow K_S^0 K^+ K^-$ decays corresponding to the two-body decay $D^0 \rightarrow K_S^0 \phi$, we have selected $K_S^0 K^+ K^-$ events with $K^+ K^-$ mass in the ϕ band defined as $1.010 < M(K^+ K^-) < 1.030 \text{ GeV}/c^2$. The unweighted and weighted $K_S^0 K^+ K^-$ mass distributions for candidate events in the ϕ region are shown in Fig. 10. There is a clear D^0 signal. Parameters for the D^0 signal from fits to the distributions of Fig. 10 are given in Table 3. No attempt has been made to correct for any small contribution from non- ϕ $K^+ K^-$ pairs which fall under the ϕ peak. The possible existence of such a contribution is under study.

Table 3. Unweighted and Weighted D^0 Signal Parameters for the ϕ Band.

parameter	unweighted	weighted
Yield	13.8 ± 4.3	364 ± 118
Mass	$1867.7 \pm 2.3 \text{ MeV}/c^2$	$1868.0 \pm 2.9 \text{ MeV}/c^2$
Width	$6.2 \pm 2.3 \text{ MeV}/c^2$	$7.1 \pm 2.6 \text{ MeV}/c^2$
Signal/Noise	2.2	2.4

Taking into account the known branching fraction $(49.5 \pm 1.0)\%$ for $\phi \rightarrow K^+ K^-$, the branching fraction for $B(D^0 \rightarrow \bar{K}^0 \phi)/B(D^0 \rightarrow K_S^0 \pi^+ \pi^-)$ is determined from the ratio of acceptance-weighted $K_S^0 \phi$ and $K_S^0 \pi^+ \pi^-$ signal yields as

$$\begin{aligned} \frac{B(D^0 \rightarrow \bar{K}^0 \phi)}{B(D^0 \rightarrow \bar{K}^0 \pi^+ \pi^-)} &= \frac{N(D^0 \rightarrow K_S^0 K^+ K^-)^{\phi cut}}{N(D^0 \rightarrow K_S^0 \pi^+ \pi^-) B(\phi \rightarrow K^+ K^-)} \\ &= 0.16 \pm 0.06 \end{aligned}$$

where again the error is statistical only. This preliminary value is consistent with the ARGUS result[11] of 0.155 ± 0.033 . If the branching ratios for $D^0 \rightarrow \bar{K}^0 \pi^+ \pi^-$ from Refs. [1] and [18] are again used, preliminary estimates are obtained for the absolute branching fraction $B(D^0 \rightarrow \bar{K}^0 \phi)$ of $(0.90 \pm 0.39)\%$ and $(1.02 \pm 0.37)\%$ in reasonable agreement with the average of the three other experiments [11] [12][13] which have reported observations of this mode: $B(D^0 \rightarrow \bar{K}^0 \phi) = (.83^{+0.18}_{-0.16})\%$ (ARGUS, CLEO, Mark III average).

A rough estimate of the $D^0 \rightarrow \bar{K}^0 K^+ K^-$ non- $\bar{K}^0 \phi$ to $D^0 \rightarrow \bar{K}^0 \pi^+ \pi^-$ branching ratio can be made by fitting the mass distributions for $K_S^0 K^+ K^-$ events excluding the ϕ region. A preliminary value from these fits is

$$\frac{B(D^0 \rightarrow \bar{K}^0 K^+ K^- \text{ non-}\bar{K}^0 \phi)}{B(D^0 \rightarrow \bar{K}^0 \pi^+ \pi^-)} = 0.15 \pm 0.05$$

where again no allowance has been made for possible small non- ϕ contributions in the ϕ band.

Other possible contributions to the $D^0 \rightarrow \bar{K}^0 K^+ K^-$ channel in addition to $\bar{K}^0 \phi$ include $\bar{K}^0 a_0(980)$ and non-resonant $\bar{K}^0 K^+ K^-$ final states[13]. To obtain better determinations for the contributions of the different modes an overall fit to the Dalitz plot for this channel is being made. In the $D^0 \rightarrow \bar{K}^0 \pi^+ \pi^-$ channel possible contributions include $K^{*-} \pi^+$, $\bar{K}^0 \rho^0$, and non-resonant $\bar{K}^0 \pi^+ \pi^-$. Fits to the Dalitz plot for this system will also be made. Most of the analysis described in this section is being done by R. W. Gardner of the University of Notre Dame.

Summary

Candidate driven charm selection algorithms have been applied to photoproduction data from the first run of Fermilab experiment E687. Several of the resulting event samples have been described including $\Lambda_c^+ \rightarrow p K^- \pi^+$, $D_s^+ \rightarrow \phi \pi^+$, $D^0 \rightarrow K_S^0 K^+ K^-$ and $D^0 \rightarrow K_S^0 \pi^+ \pi^-$ decays. Preliminary lifetime values for the Λ_c^+ and D_s^+ are presented. Preliminary values for some D^0 branching ratios are given.

Acknowledgements

We wish to acknowledge the assistance of the staffs of Fermilab, INFN of Italy and the physics departments of the University of Colorado, University of Illinois, Northwestern University, and Notre Dame University. This research was supported in part by the National Science Foundation, the U.S. Department of Energy, the Italian Istituto Nazionale di Fisica Nucleare and Ministero della Universita' e della Ricerca Scientifica.

Footnotes

- (*a*) Present address: IBM TJ Watson Laboratories, Yorktown Heights, NY 10598
- (*b*) Present address: University of Oklahoma, Norman, OK 73019, USA
- (*c*) Present address: University of North Carolina, Ashville, NC 28804, USA
- (*d*) Present address: Fermilab, Batavia, IL 60510, USA
- (*e*) Present address: Dipartimento di Elettronica, Universita' di Pavia, Pavia, Italy
- (*f*) Present address: Universita di Pavia and INFN, I-27100 Pavia, Italy
- (*g*) Present address: University of Alabama, Tuscaloosa, AL 35487, USA

References

- [1] G.P. Yost *et al.* (Particle Data Group), *Phys. Lett.* **B204**, 1 (1988).
- [2] R.J. Morrison and M.S. Witherell, *Ann. Rev. Nucl. Part. Sci.* 1989 **39**, 183.
- [3] "*D*⁺, *D*⁰ Signals and Lifetimes in E687 Photoproduction Experiment at Fermilab", submitted to this conference by L. Moroni for the Fermilab E687 Collaboration.
- [4] I.I. Bigi and M. Fukugita, *Phys. Lett.* **B91**, 121 (1980).
- [5] J. Wilson for the E687 Collaboration, *Proceedings of the 1990 DPF Meeting*, Houston, TX, (to be published).
- [6] "Description of the E687 Spectrometer", submitted to this conference by S. Gourlay for the Fermilab E687 Collaboration.
- [7] P.L. Frabetti *et al.* "Description and Performance of the E687 Spectrometer", to be submitted to *Nuclear Instruments and Methods*.
- [8] J.C. Anjos *et al.*, *Phys. Rev. Lett.* **60**, 1379 (1988).
- [9] C.W. Bogart, Ph.D. Dissertation, University of Colorado (1990) (unpublished).
- [10] N. Cason and R. Cunningham, "Study of Background Distributions in the $\phi\pi$ Final State" Notre Dame HEP internal memo (March, 1990) (unpublished).
- [11] H. Albrecht *et al.*, *Phys. Lett.* **B158**, 525 (1985).
- [12] C. Bebek *et al.*, *Phys. Rev. Lett.* **56**, 1983 (1986).
- [13] R.M. Baltrusaitis *et al.*, *Phys. Rev. Lett.* **56**, 2136 (1986).
- [14] S. Barlag *et al.*, CERN EP/90-47 (April 9, 1990), submitted to *Z. Phys. C*.

- [15] B. Blok and M.A. Shifman, *Yad. Fiz.* **45**,211,478,841 (1987).
- [16] M. Bauer, B. Stech, and M. Wirbel, *Z. Phys.* **C34**, 103, (1987).
- [17] A.J. Buras, J.M. Gerard, and R. Ruckl, *Nucl. Phys.* **268**, 16 (1986).
- [18] J. Adler *et al.*, *Phys. Lett.* **B196**, 107 (1987).

Figure Captions

- Fig. 1 Effective mass distribution for accepted $pK^- \pi^+$ and charge conjugate combinations after all cuts. The curve is a fit with a Gaussian signal plus a quadratic background as described in the text.
- Fig. 2 Distribution in corrected proper time $t' = (L - 3.0\sigma_L)/\beta\gamma c$ for $\Lambda_c^+ \rightarrow pK^- \pi^+$ candidates with masses between 2.10 and 2.45 GeV/c^2 . The curve is a fit described in the text.
- Fig. 3 The effective mass distribution for $K^+ K^-$ combinations where both tracks are Čerenkov consistent with the kaon hypothesis. The curve is a fit with a P-wave Breit-Wigner signal function for the ϕ and a second-order polynomial background.
- Fig. 4 Distributions of $\phi\pi$ mass for different cuts on L/σ_L . The curves are fits with Gaussian signals for the D^+ and D_s^+ and a linear background term.
- Fig. 5 The binned distribution in proper time t for $\phi\pi$ candidates with masses in the narrow D_s^+ mass region from 1.94 to 1.99 GeV/c^2 . The curve is a fit described in the text. The effects of the L/σ_L cut can be seen at small t .
- Fig. 6 The K_S^0 mass distribution for the event sample used as a starting point for $D^0 \rightarrow K_S^0 K^+ K^-$ and $D^0 \rightarrow K_S^0 \pi^+ \pi^-$ candidate selection.
- Fig. 7 Unweighted distributions of $K_S^0 \pi^+ \pi^-$ and $K_S^0 K^+ K^-$ effective mass for D^0 decay candidates with $L/\sigma_L > 3.0$. The fits are described in the text.
- Fig. 8 Weighted distributions of $K_S^0 \pi^+ \pi^-$ and $K_S^0 K^+ K^-$ effective mass for D^0 decay candidates with $L/\sigma_L > 3.0$. The fits are described in the text.
- Fig. 9 The two-dimensional scatter plot of $K^+ K^-$ mass as a function of the candidate $K_S^0 K^+ K^-$ mass for the total $K_S^0 K^+ K^-$ sample (a) together with the corresponding unweighted $K_S^0 K^+ K^-$ (b) and $K^+ K^-$ (c) mass distributions.
- Fig.10 Unweighted and weighted $K_S^0 K^+ K^-$ mass distributions for D^0 candidates in the ϕ region. The fits are described in the text.

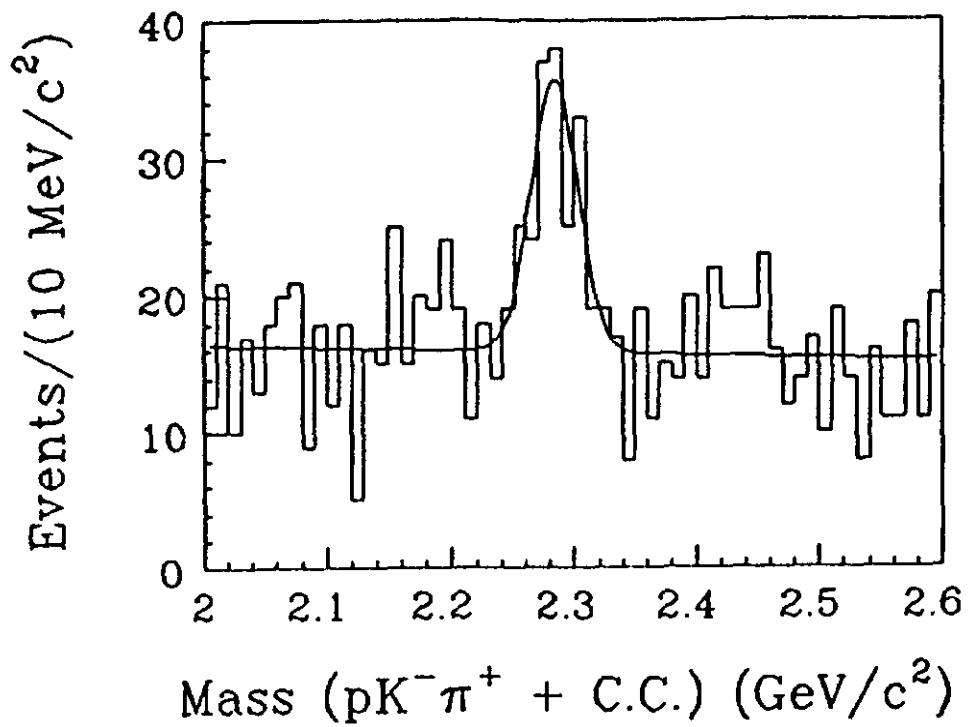


Fig. 1

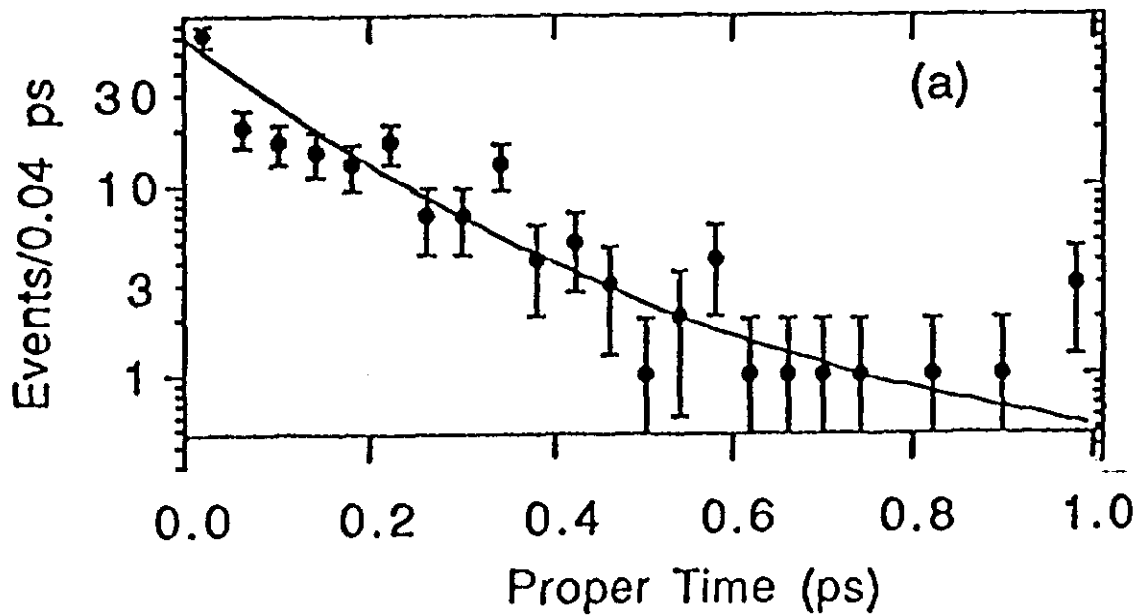


Fig. 2

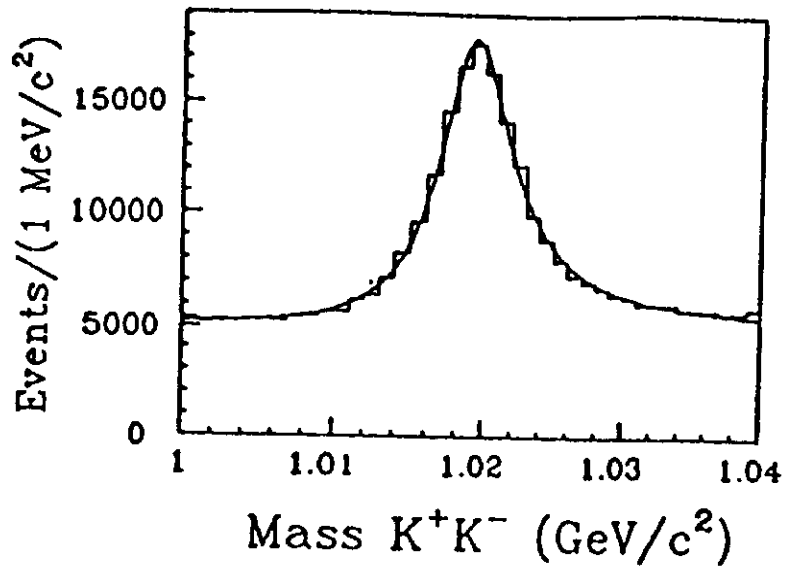


Fig. 3

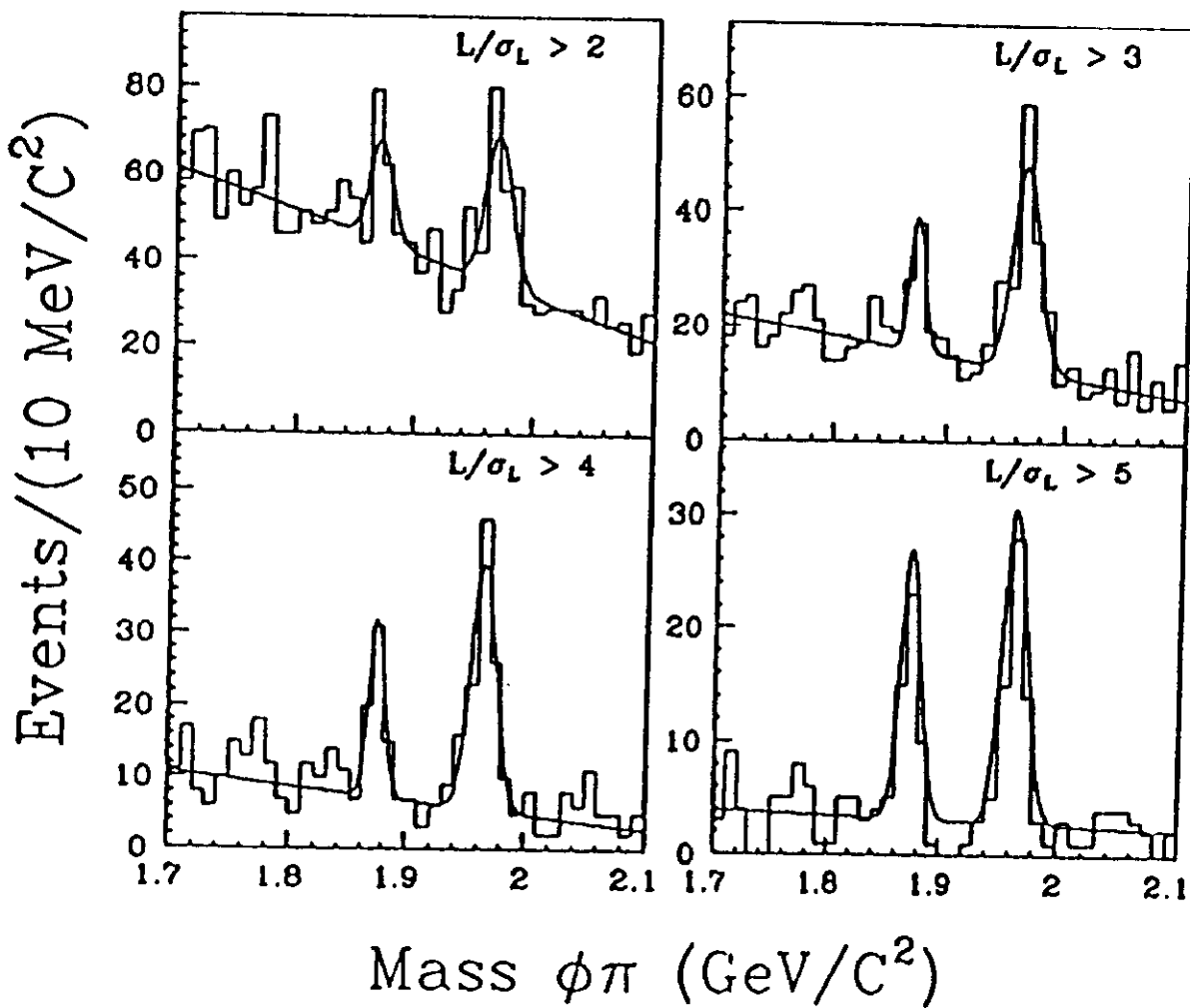


Fig. 4

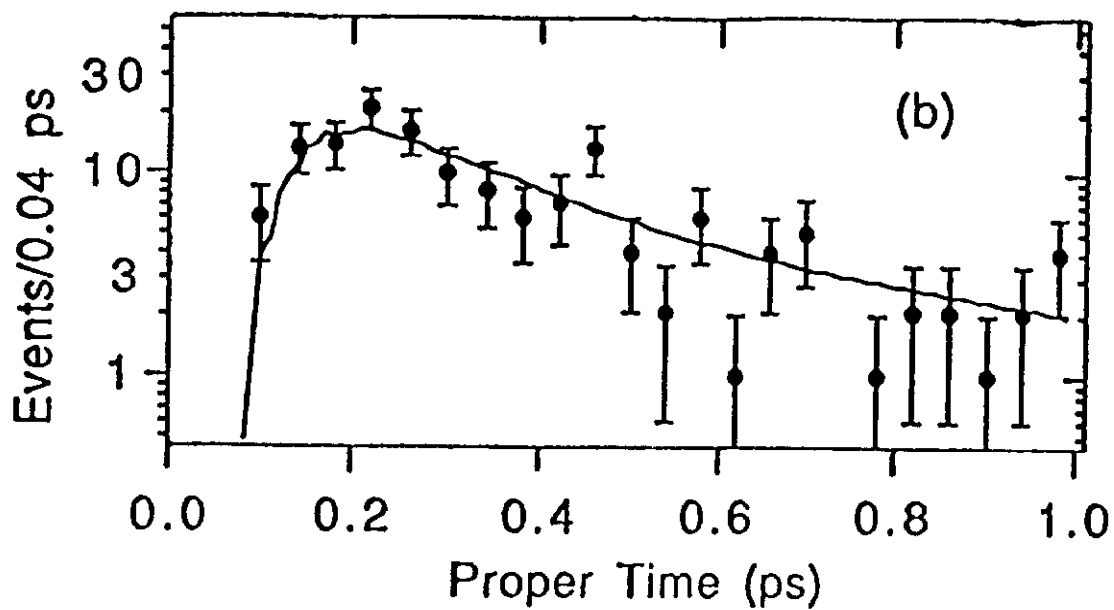


Fig. 5

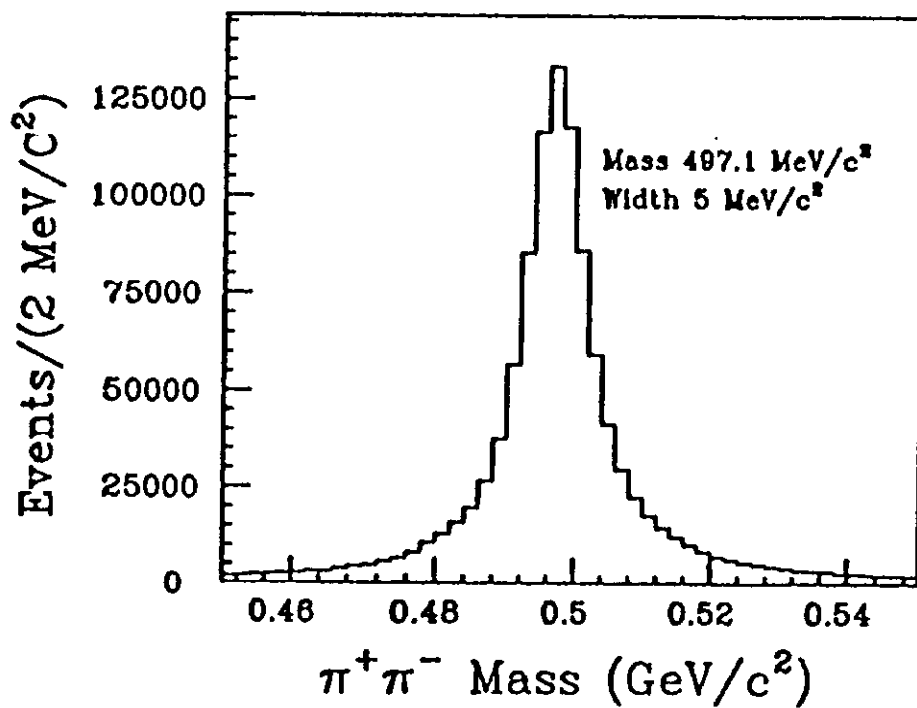


Fig. 6

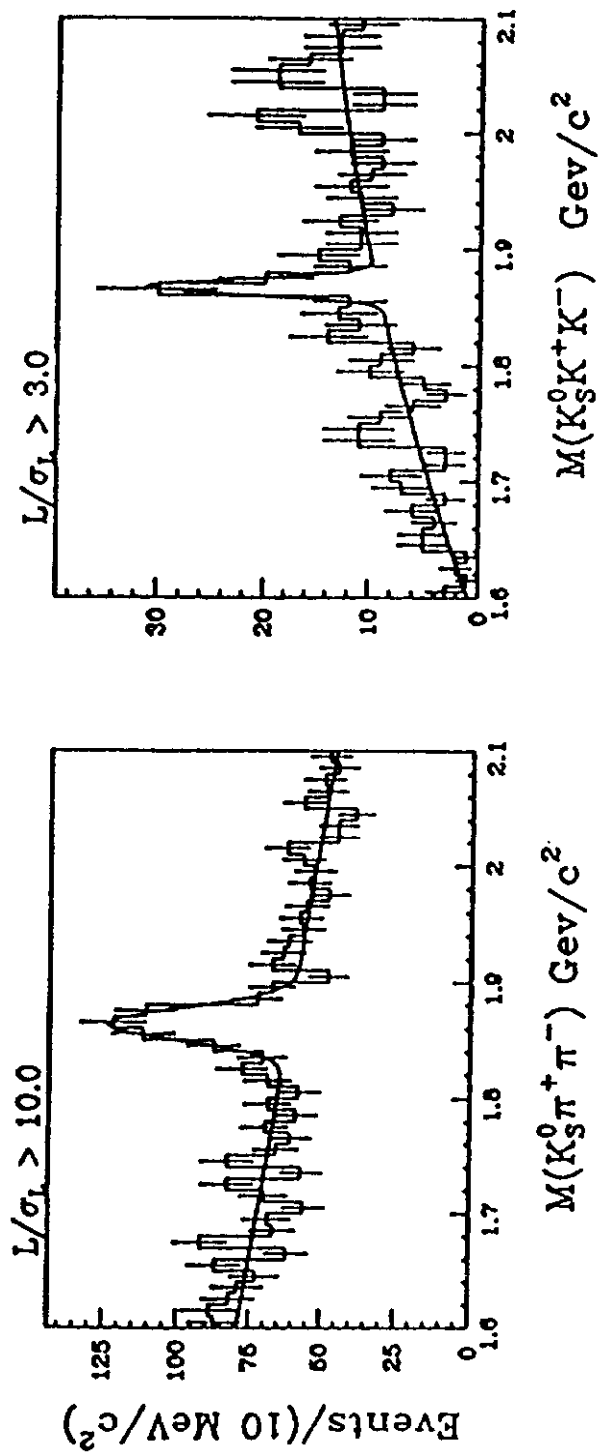


Fig. 7

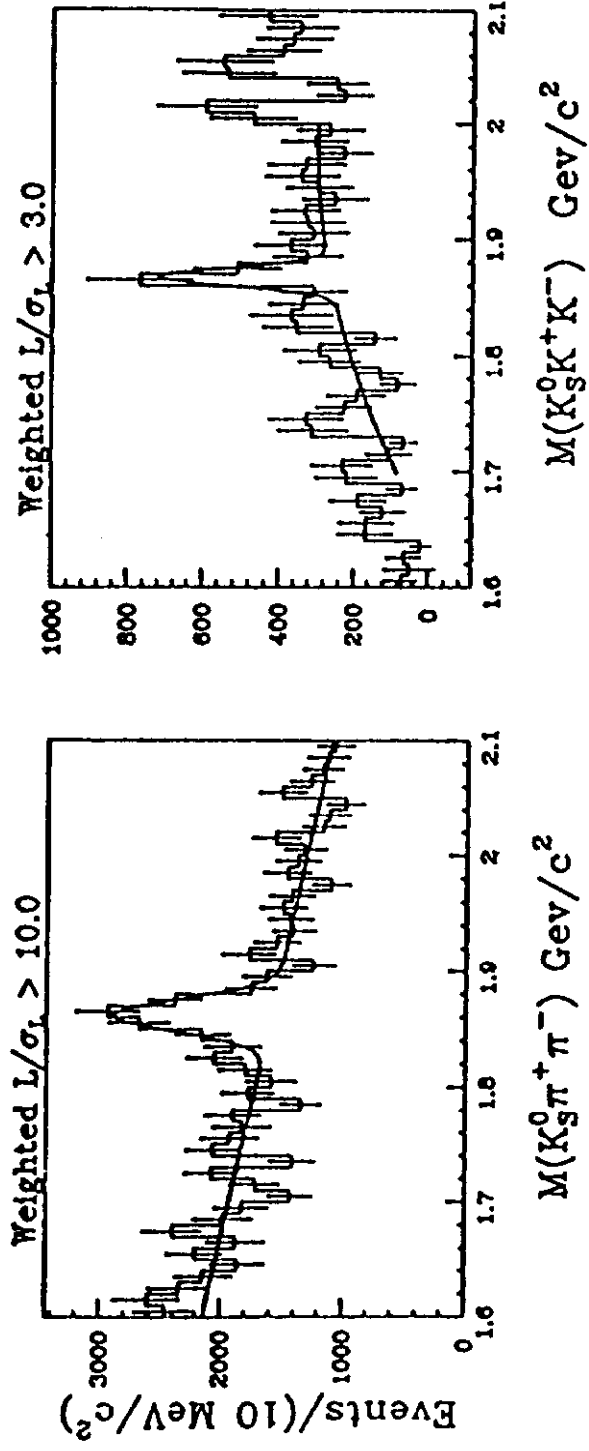
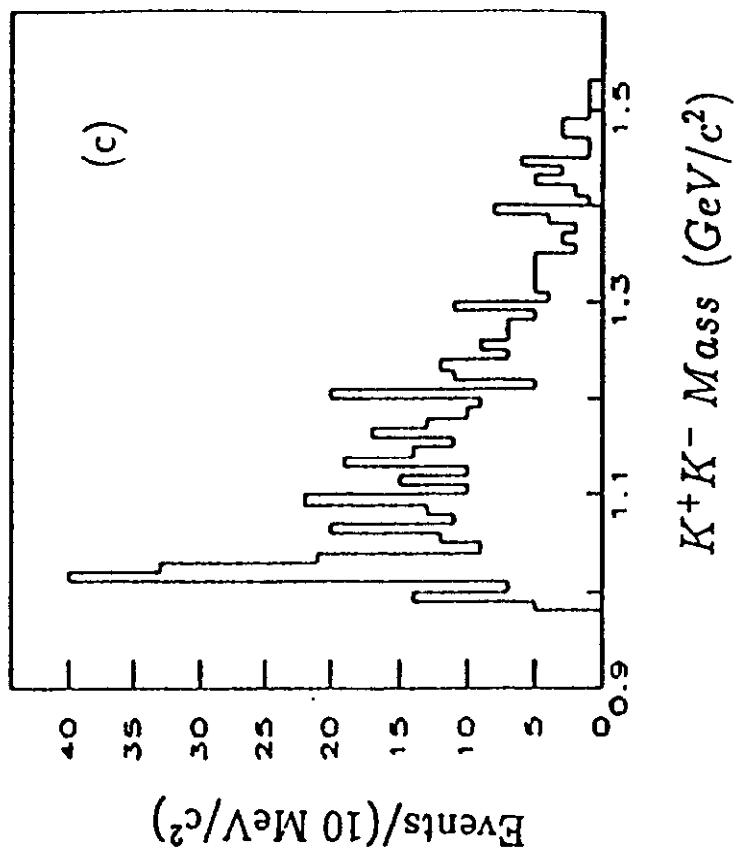
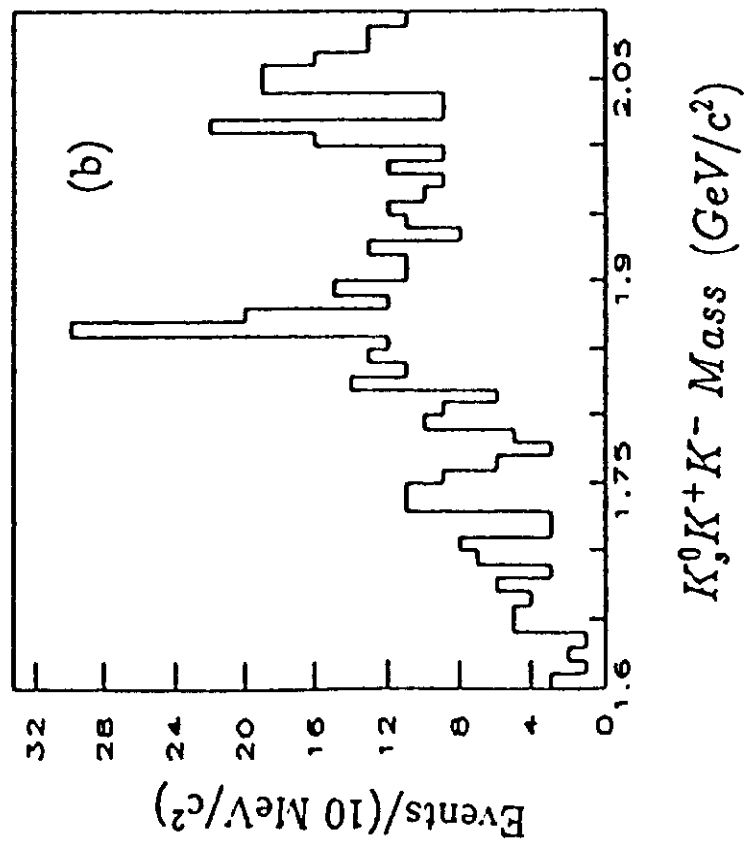
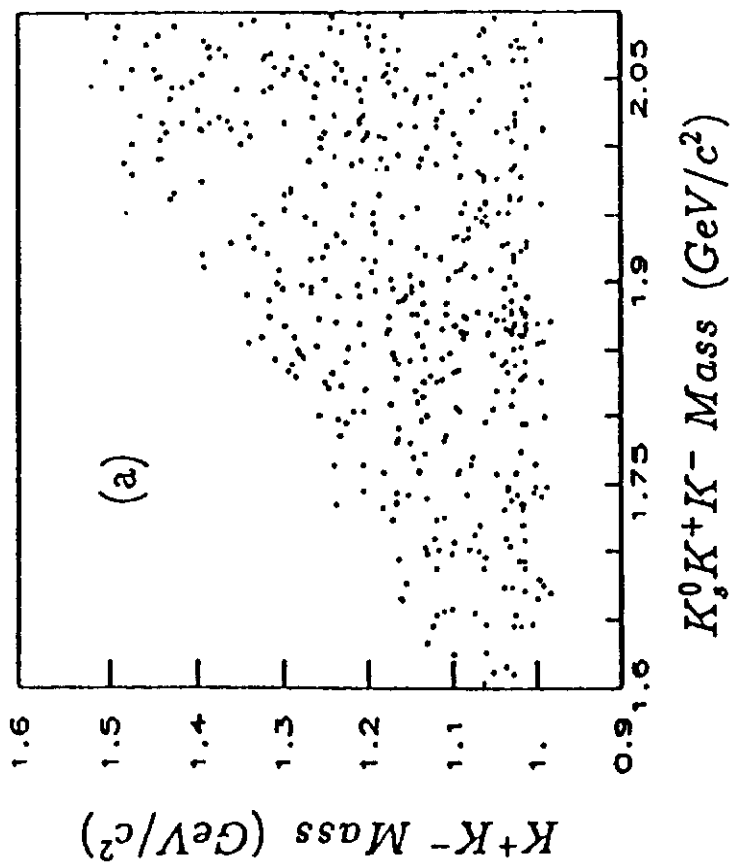


Fig. 8

Fig. 9



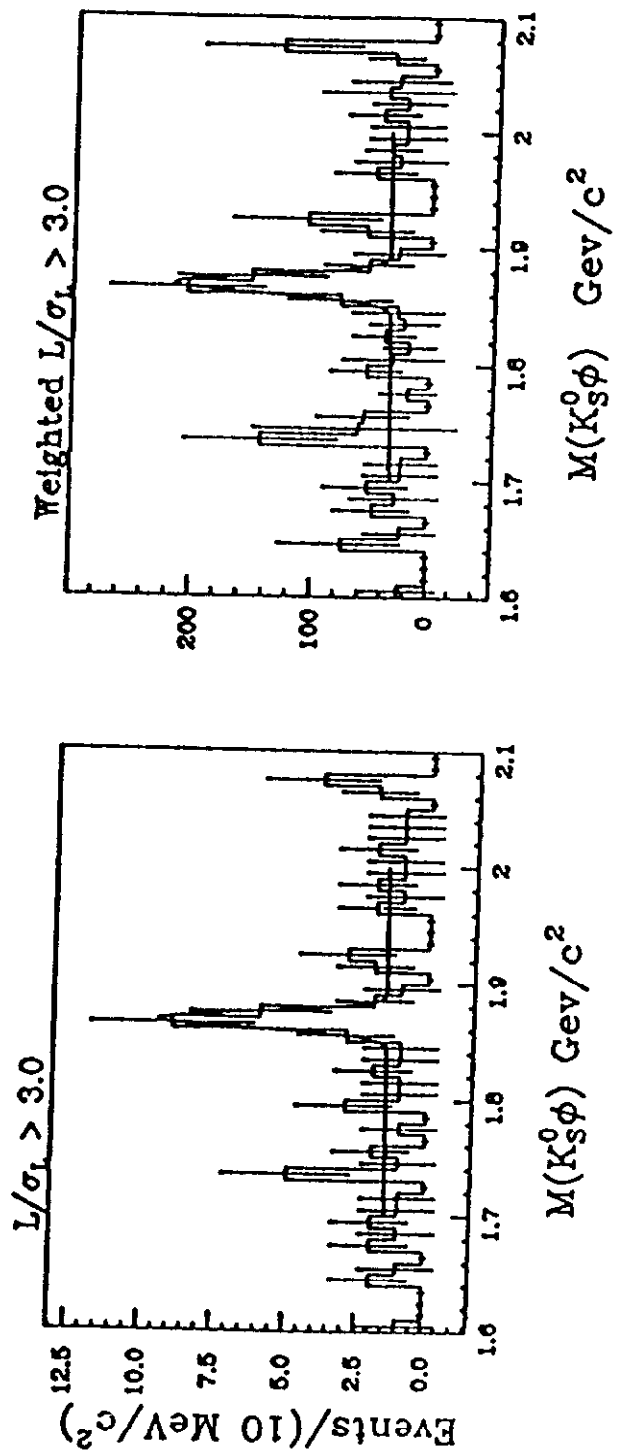


Fig. 10